Available online at www.sciencedirect.com
ScienceDirect
Colloids and Surfaces A: Physicochem. Eng. Aspects 287 (2006) 175–181
COLLOIDS AND SURFACES A
www.elsevier.com/locate/colsurfa

Nanostructured and chemically modified hydrophobic polyolefin surfaces

Esa Puukilainen [a], Hanna-Kaisa Koponen [a], Zhili Xiao [b,c], Sari Suvanto [a], Tapani A. Pakkanen [a,*]

[a] *Department of Chemistry, University of Joensuu, P.O. Box 111, Fin-80101, Joensuu, Finland*
[b] *Materials Science Division, Argonne National Laboratory, Argonne, IL 60439, USA*
[c] *Department of Physics, Northern Illinois University, DeKalb, IL 60115, USA*

Received 12 December 2005; received in revised form 7 March 2006; accepted 28 March 2006
Available online 15 April 2006

Abstract

Hydrophobic polyolefin (PO) surfaces were prepared by perfluoropolyether (PFPE) blending and nanostructuring. Surface modifications were done by injection molding. Two high-density polyethylenes and polypropylene were melt blended with 2.0 wt.% of PFPE. Both polyethylenes formed blends with PFPE and showed improved hydrophobicity. For nanostructuring, self-ordered nanoporous mold inserts were fabricated by anodizing aluminum in polyprotic acid. Nanostructured samples were prepared with nanoporous anodic aluminum oxide masks from pure polyolefins and from PO/PFPE blends containing 2 wt.% PFPE. Nanostructuring had a marked effect on the contact angle between injection moldable polyolefins and water: well-arranged, high aspect ratio nanostructure was found over the entire surface.

Keywords: Polyolefin; Perfluoropolyether (PFPE); Nanoporous anodic aluminum oxide (AAO); Nanostructuring by injection molding

1. Introduction

Nature produces amazing surfaces for scientists to mimic. Butterfly wings [1] and leaves of the lotus plant [2,3] are good examples. Color, UV protection, super hydrophobicity, and self-cleaning ability are produced on these surfaces through a combination of specific surface chemistry and highly organized surface structure [1–3]. Several methods have been introduced for preparation of artificial surfaces with surface properties such as super hydrophobicity. Plasma and chemical vapor deposition (CVD) treatments are the methods most often employed [4–8]. Other methods successfully applied include crystallization of melted or solution-cast compounds on a substrate, typically a glass plate [9,10], living free radical polymerization [11], and molding of a sol–gel [12,13]. Lithography [14–16], laser treatment [17,18], and reactive blending of polymers in a twin-screw extruder [19] are also workable methods in the preparation of super hydrophobic, self-cleaning surfaces. Ebbens and Badyal [20] prepared fluorochemical-doped polypropylene films by melt blowing. With several surface-sensitive techniques they monitored the migration of fluorochemical additive toward the surface of polypropylene film during the annealing. By annealing the film at 130 °C just 15 min they were successful to prepare a film with a continuous, low surface energy, additive layer. The limitation for most of these techniques is that it is very difficult to control the formation of the surface structure; additionally, they are suitable only for planar surfaces and surfaces of limited size.

Polyolefins (PO) are the world's richest tonnage thermoplastics and are widely used in applications where hydrophobicity and clean surfaces are required [21]. We recently demonstrated that the hydrophobicity of high-density polyethylene (HDPE) can be permanently improved by melt blending with perfluoropolyethers [22]. Perfluoropolyethers (PFPEs) are a class of low molecular mass polymers characterized by exceptional stability. PFPEs are used in extreme conditions and in exotic applications where special properties are needed, for example as lubricants in computer hard disks [23]. A short introduction to these materials can be found in our earlier paper [22].

Fabrication of an organized nanostructure on the surface of chemically modified polyolefin should make the polyolefin

* Corresponding author. Tel.: +358 13 2513345; fax: +358 13 2513344.
E-mail address: Tapani.Pakkanen@joensuu.fi (T.A. Pakkanen).

0927-7757/$ – see front matter © 2006 Elsevier B.V. All rights reserved.
doi:10.1016/j.colsurfa.2006.03.056

still more hydrophobic, approaching an artificial self-cleaning surface. Nanoporous anodic aluminum oxide (AAO) has a self-ordered porous structure consisting of close-packed hexagonal cells, each with a nanopore in the center. AAO is fabricated by anodizing aluminum in polyprotic acids [24]. A porous structure forms during anodization, and the two-step anodization process demonstrated by Masuda and Satoh [25] gives a triangularly ordered structure through the film [26,27]. The diameters of the pores and interpore distances can be tuned by choice of the electrolyte and anodization voltage [28,29]. Thanks to the uniform diameter and spacing of the pores, AAO template synthesis is widely used as a low cost method to fabricate nanostructures such as dots [25,30,31], wires and rods [32,33], and tubes [34–37] in high yield. Nanopillars on surfaces imprinted with use of AAO as a mask affect the optical reflectivity and wettability of materials [38,39]. Naturally occurring self-ordering enables economical fabrication of large-area structures with high aspect ratios by injection molding, unlike the lithographic techniques conventionally used in the nanopatterning of surfaces.

In previous work, we demonstrated that melt blending HDPE with PFPE permanently improves the hydrophobicity of the polyethylene [22]. The aim of the present work was to explore the possibility of preparing polyolefin surfaces that are simultaneously chemically and structurally modified. The modifications were designed to produce a material with a specific surface chemistry and controlled surface nanostructure. If successful, the surfaces would have permanently improved properties, particularly hydrophobicity, allowing a broader use of polyolefins. Modifications were done by injection molding: liquid PFPE was added to the melt polyolefin and an AAO mold insert was used to nanopattern the surfaces. The chemical composition of the mixtures and the relative amount of PFPE on the surface were studied by ATR-IR spectroscopy and the nature of the surface, especially its hydrophobicity, was studied by measuring the contact angle between the surface and water. Structures of the nanopatterned surfaces were examined by SEM imaging.

2. Experimental

2.1. Materials and methods

Polyolefins were Borealis' high-density polyethylene (BL 2631) recommended for blow molding, density 963 kg/m^3; high density polyethylene 1-butene copolymer (MB 7541) recommended for injection molding, density 954 kg/m^3; and polypropylene homopolymer (HD 120 MO) recommended for injection molding, density 908 kg/m^3. For simplicity, BL 2631 is designated PE, MB 7541 is designated bPE, and HD 120 MO is designated PP. Perfluoropolyether was Fomblin® Y06 from Ausimont. Fomblin® Y06 is an unfunctionalized perfluoropolyether with molecular mass 1800 AMU, and it is termed PFPE.

Blended polyolefin samples were made by injection molding with a DSM Midi 2000 extruder—microinjection-molding machine. The following processing parameters were selected on the basis of previous research [22] (the first value for polyethylenes and then the value for polypropylene): screw temperature 225 °C/255 °C, mold temperature 40 °C/50 °C, and screw rotation speed 100 rpm/80 rpm. PFPE was injected with a glass capillary pipette to the barrel of the extruder and into liquid PO so that the amount of injected PFPE was 2.0 wt.%. Nanostructured samples were prepared by the same method but with an AAO mold insert inserted into the injection mold.

Infrared spectroscopic (IR) measurements were carried out with a Nicolet Avatar 320 FTIR spectrometer. An attenuated total reflectance (ATR) accessory was used to examine the surfaces of the PO/PFPE samples. In the ATR technique, the IR radiation penetrates a few micrometers into the sample [40], giving information about the composition of the sample from a relatively thick layer. Three parallel measurements were made of each sample and average spectra were calculated for each of the polyolefins.

Contact angle measurements were carried out with a KSV Cam 200 contact angle meter. Contact angle measurement is an accurate method for determining the interaction energy between a liquid and a solid. The wettability of a solid surface strongly depends on its surface structure [41–47]. Static contact angle measurements were made at room temperature with ion exchanged water. A drop of water (5 μl) was placed on the sample and photographed once a second for 30 s. The contact angle was determined mathematically by fitting a Young-Laplace curve around the drop. Values recorded between 6 and 30 s were averaged to obtain the contact angle for each measurement. Nine parallel measurements were made of each sample, and average contact angle values were calculated for each polyolefin.

The surface structure of the samples was studied with a Hitachi S4800 FE-SEM, equipped with upper and lower (semi-in-lens) secondary electron (SE) detectors. The samples were mounted onto a stub with copper adhesive tape and coated with 2 nm of Pt/Pd. Accelerating voltages of 2–3 kV and a general working distance of 8 mm was applied.

2.2. Fabrication of AAO masks

A piece of an aluminum foil (Alfa Aesar, 0.25-mm thick, Puratronic, 99.997%,) 3 cm × 3.5 cm was degreased in acetone and electropolished in a mixture of perchloric acid and ethanol (1:8) using platinum foil as a counter-electrode. The electropolishing current was 2.7 A and the time was 135 s. The foil was then rinsed with deionized water and allowed to dry at room temperature.

The back-side of the dry and electropolished aluminum foil was protected against anodization with nail polish (Maybelline Foreverstrong + iron). The nail polish was applied so as to extend above the electrolyte solution but it was not allowed to cover the foil under the fasteners. Anodization was carried out at a constant voltage (40 or 60 V) in 0.3 M oxalic acid, at 3 °C for 24 h.

After anodization the protective nail polish layer on the back-side was removed with acetone, and the anodized side was covered with nail polish to protect it during removal of the unreacted aluminum and barrier layer. The native oxide layer was removed from the aluminum surface with 10% NaOH, after which unreacted aluminum was removed with 0.5 M $CuCl_2$

solution by rubbing with a cotton stick. Addition of two or three drops of HCl to the $CuCl_2$ facilitates the removal. The barrier layer was removed with 5% H_3PO_4 solution at 30 °C. AAO membranes anodized at 40 V were soaked in phosphoric acid for 80 min and AAO membranes anodized at 60 V were soaked for 100 min. After barrier layer removal the nail polish covering was removed with acetone and the mask was soaked in deionized water for about 30 min to prevent the corrosion of the pore walls.

AAO mold inserts used in polymer patterning were fabricated by gluing the AAO membrane onto a 0.5-mm thick steel plate with heat-stable epoxy glue (Loctite® Hysol® 9492 A&B). The side from which the barrier layer was removed and where the structure was more ordered was facing upwards. For simplicity, the AAO membrane anodized at 40 V and inserted into the injection mold is called the A mask. Correspondingly, the AAO membrane anodized at 60 V is called the B mask.

3. Results and discussion

3.1. Processing and characterization of PO/PFPE blends

3.1.1. Analysis of surface composition by ATR-FTIR measurements

ATR-FTIR measurements were used to determine the relative amount of PFPE on the surface of the polyolefin samples. The measurements were made both for the flat surfaces as well as for the nanostructured surfaces. Fig. 1A shows the average spectra of the polyolefins. The average spectra of the two polyethylenes were scaled so that the intensity of the C–H bending band of the CH_2 groups at 1460 cm^{-1} was the same in the two spectra. Absorption from PFPE was integrated between 1285 and 1215 cm^{-1} and the peak area was plotted together with the results for HDPE obtained in previous work [22], as shown in Fig. 1B.

The results of the ATR-IR measurements (Fig. 1A) show that both polyethylenes form blends with PFPE, but polypropylene does not. There were no differences in IR spectra between the flat surfaces and the nanostructured surfaces in any polyolefins.

3.1.2. Contact angle measurements

Table 1 shows the average contact angles and standard deviations for the three polyolefins. Fig. 2 shows the increment of the average contact angle of polyolefins with added PFPE plotted together with results for HDPE obtained previously [22].

Table 1
Average contact angle (CA) and standard deviation (S.D.) for polyolefins and PO/PFPE blends

Material	CA	S.D.
bPE	99.1	1.2
bPE + PFPE	109.0	1.1
PE	98.2	0.6
PE + PFPE	106.2	1.0
PP	102.6	1.2
PP + PFPE	107.5	1.4

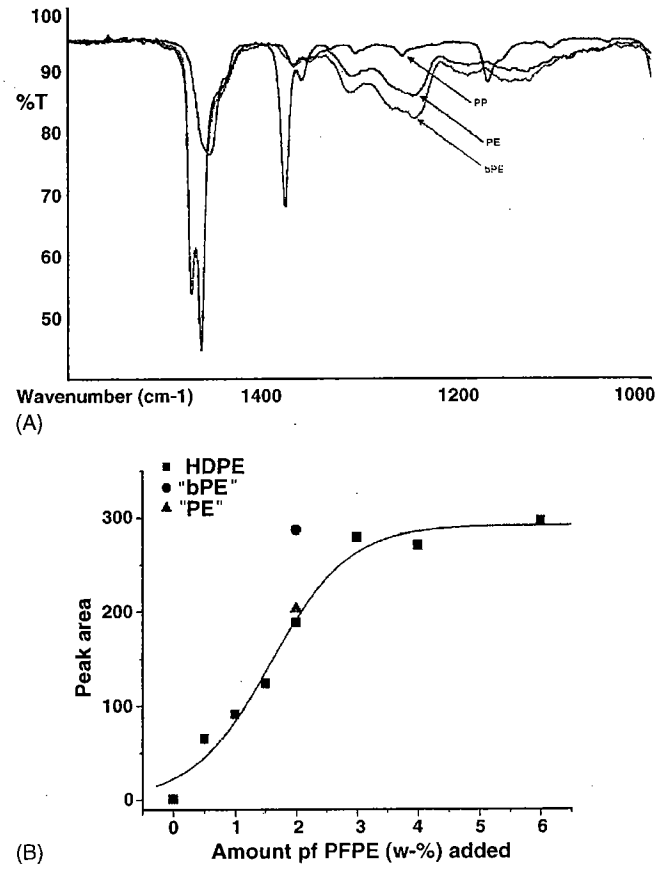

Fig. 1. (A) IR spectra of the polyolefins and (B) average peak area between 1285 and 1215 cm^{-1} recorded from polyethylenes blended with 2.0 wt.% PFPE, plotted with the results obtained for HDPE in previous work [22].

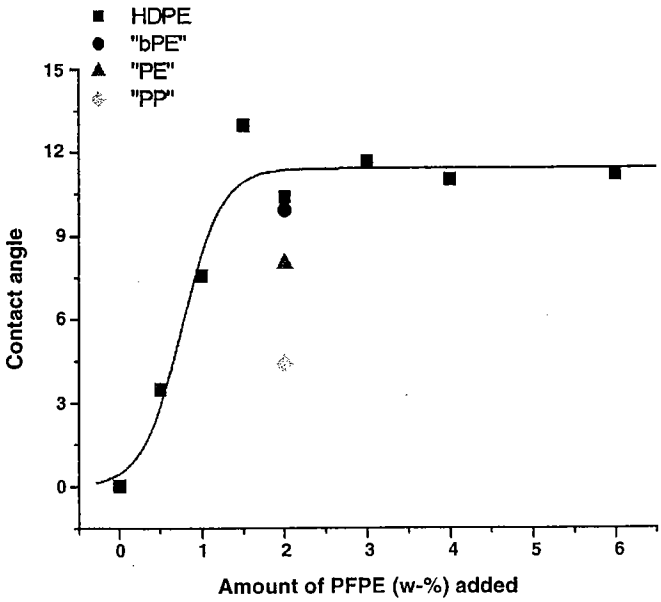

Fig. 2. Increment of the average contact angle of polyolefins with added PFPE plotted with the results for HDPE obtained in previous work [22].

When 2 wt.% of PFPE was added to the polyethylenes the value of the average contact angle increased by 8 and about 10°. With the same amount of PFPE added to the polypropylene, the increase was only about 5°. The findings are in agreement with those obtained by ATR-IR spectroscopy, namely, both polyethylenes form blends with PFPE, but polypropylene does not.

3.2. Fabricated AAO masks

Anodization was carried out in a single step, so that only one side of the AAO membrane had an ordered structure after barrier layer removal. The pore walls were corroded during barrier layer removal, and the pore diameters were tuned by adjustment of the removal time. The interpore distances remained constant and only the wall thickness between pores was diminished by increasing the processing time. An ordered structure on just one side was sufficient because the AAO membrane was used as a mask.

Anodization voltage affected the ordering of the porous structure. The A mask, which was prepared with lower voltage had the most ordered triangular structure with interpore distances of 100–120 nm. While for the B mask, the triangular ordering of the pores was poorer and distribution of the interpore distances was wider, being 130–190 nm. Fig. 3 shows SEM images of the AAO masks. The A mask was imaged after injection molding and the B mask before injection molding. As can be seen from the SEM images, injection molding has no effect on the masks.

3.3. Nanostructured polyolefins

Nanostructured polyolefins and PO/PFPE blends were prepared by injection molding, and the surface structures were examined by contact angle measurements and SEM imaging. Samples were made, with both A and B masks, from pure polyolefins and from PO/PFPE blends containing 2 wt.% Fomblin® Y06. 0.6-mm thick A and B masks were inserted into the 2.0-mm-high injection mold cavity and nanostructured samples were removed from the mold manually.

3.3.1. Contact angle measurements

Static contact angle measurements of nanostructured surfaces were made with the method for flat surfaces. Contact angle hysteresis of different surface types was obtained by measuring contact angles of increasing and decreasing water drop volume. Dynamic contact angle measurements were carried out with an automatic dispenser, and contact angles were measured between drop volumes 2.5 and 7.0 μl.

Eq. (1) shows the relationship according to Wentzel [41] between a flat surface contact angle and a rough surface contact angle:

$$\cos \theta^* = r \cos \theta, \tag{1}$$

where θ^* is the apparent contact angle, r the roughness factor (defined as actual surface divided by geometric surface), and θ the Young's angle. Since $r > 1$, both hydrophobicity and hydrophilicity are intensified by roughness. A few years after Wentzel introduced his equation, Cassie and Baxter introduced their theory of wettability of porous surfaces [42]. The Cassie-Baxter relation is shown in Eq. (2):

$$\cos \theta^* = \phi_s(1 + \cos \theta) - 1, \tag{2}$$

where θ^* is the apparent contact angle, ϕ_s an area fraction of solid surface, and θ the Young's angle. Comparative study on the Wentzel and Cassie-Baxter theories commenced with Johnson Jr. and Dettre [43]. They and others [43–47] found that the Wentzel model works with surfaces of moderate surface roughness and when the contact angle hysteresis is large, while the Cassie-Baxter model works with rougher surfaces and when contact angle hysteresis is low.

All nanostructured surfaces showed clear hydrophobicity (110–133°) and all surface types only moderate contact angle hysteresis (about 25°). In view of these findings, we applied the Cassie-Baxter equation to compare the results of our contact angle measurements. Contact angle measurements of flat pure polyolefins and PO/PFPE blends showed the surfaces to be homogeneous (S.D. ~1°). Moreover, SEM images of flat pure polyolefins and PO/PFPE blends showed no surface nanostructures. Accordingly, contact angles of flat pure polyolefins and

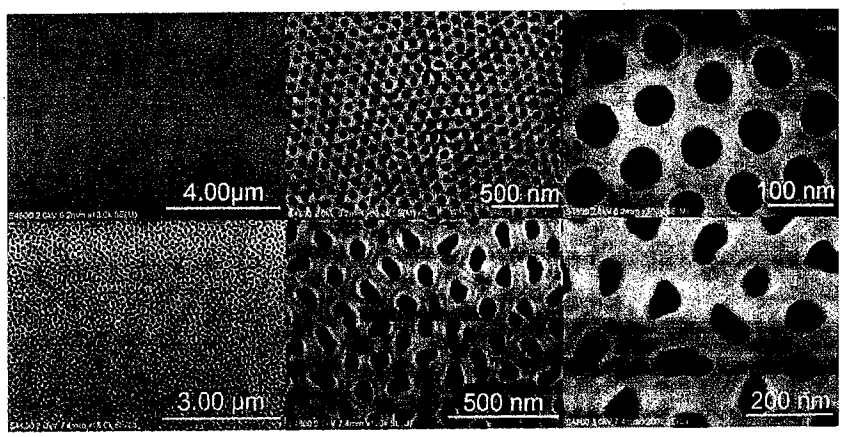

Fig. 3. SEM images of AAO masks: A mask (top) after injection molding and B mask (below) before injection molding.

Table 2
Contact angle (CA), standard deviation of CA (S.D.), and calculated solid fraction of the surface (ϕ_s) for polyolefin and PO/PFPE blend surfaces

Material	CA	S.D.	ϕ_s
bPE	99.1	1.2	1.00
bPE with A mask	132.8	12.0	0.38
bPE with B mask	113.5	10.5	0.71
bPE + PFPE	109.0	1.1	1.00
bPE + PFPE with A mask	135.1	3.3	0.43
bPE + PFPE with B mask	126.3	12.0	0.61
PE	98.2	0.6	1.00
PE with A mask	122.3	11.3	0.54
PE with B mask	114.8	16.6	0.68
PE + PFPE	106.2	1.0	1.00
PE + PFPE with A mask	113.7	3.8	0.83
PE + PFPE with B mask	123.5	11.8	0.62
PP	102.6	1.2	1.00
PP with A mask	128.4	15.2	0.48
PP with B mask	108.8	5.5	0.87
PP + PFPE	107.5	1.4	1.00
PP + PFPE with A mask	121.3	8.0	0.69
PP + PFPE with B mask	110.3	10.3	0.93

PO/PFPE blends were treated as Young's contact angles, and the solid fractions of the surfaces were set to 1.00. Table 2 shows the average contact angle, standard deviation, and calculated solid fraction of surface for all surfaces. Fig. 4 shows the solid fraction of nanostructured surfaces.

The contact angle measurements showed that surfaces patterned with the A mask have a lower solid fraction of surface than those molded with the B mask. In most cases the addition of PFPE to polyolefins increased the solid fraction of the surface, which is, of course, an unfavorable result when the aim is to produce hydrophobic nanostructured surfaces. Nanostructuring had a marked effect on the contact angle between polyolefins and water, especially with the A mask, where the contact angle increased by about 25% an average. At the same time the solid fraction of the surfaces decreased to an average about 0.5.

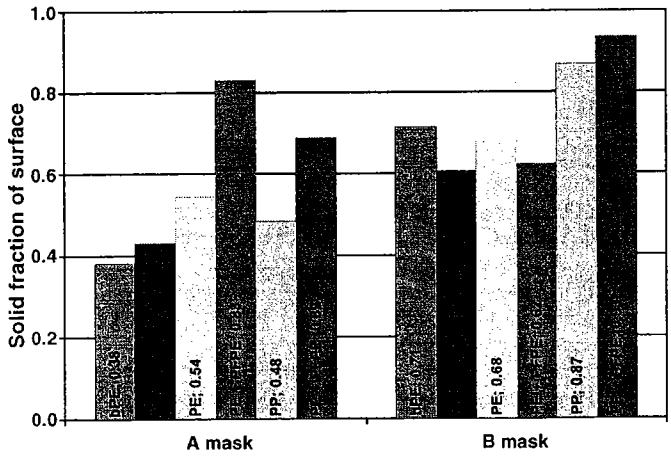

Fig. 4. Solid fraction of nanostructured surfaces of polyolefins and PO/PFPE blends.

3.3.2. *Imaging nanostructured surfaces by scanning electron microscopy*

SEM imaging was done on selected surfaces to determine the real surface structure and to confirm results of contact angle measurements. Fig. 5 shows SEM images of bPE with A mask (A & B), bPE with B mask (C & D), PP with A mask (E & F), PP + PFPE with A mask (G & H), PP with B mask (I & J),

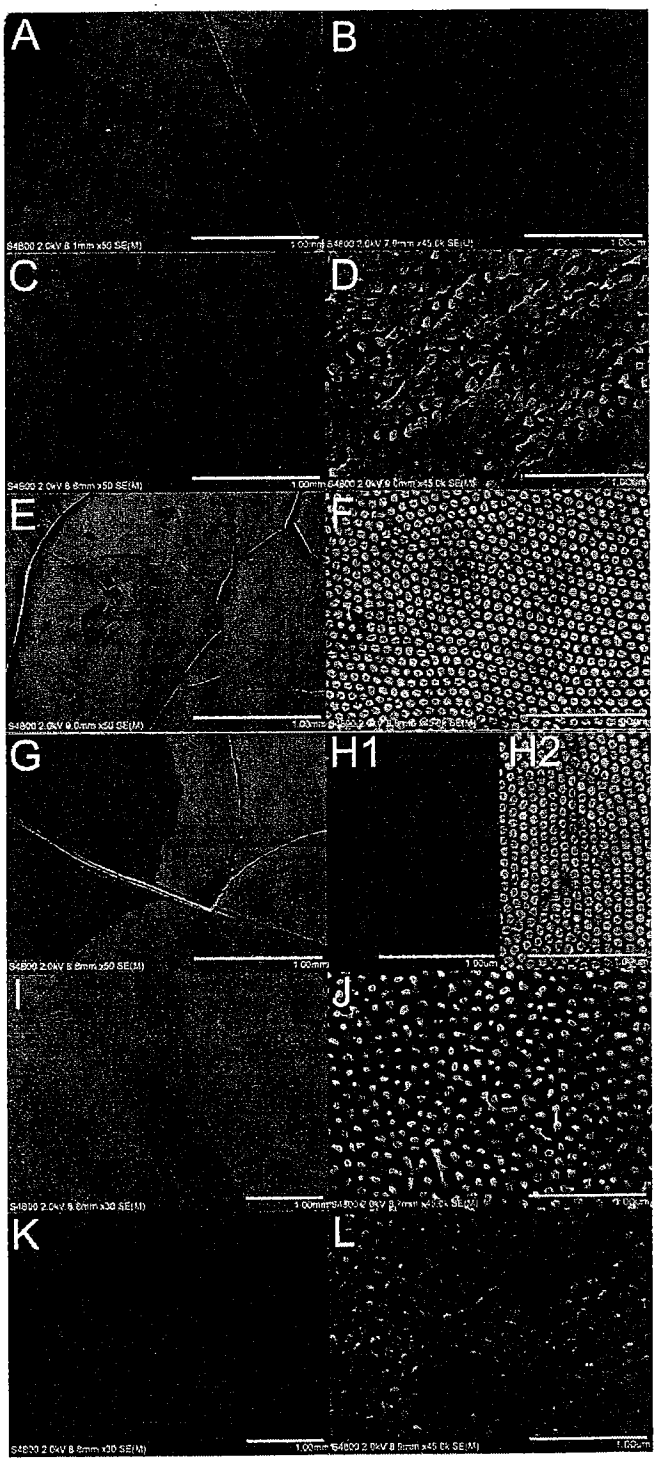

Fig. 5. SEM images of bPE with A mask (A & B), bPE with B mask (C & D), PP with A mask (E & F), PP + PFPE with A mask (G & H), PP with B mask (I & J), and PP + PFPE with B mask (K & L). Magnifications 50× (30×) on the left and 45,000× on the right; bars 1.00 mm and 1.00 μm, respectively.

and PP + PFPE with B mask (K & L) surfaces. Magnifications were 50× (30× in I & K), and 45,000×, and bars 1.00 mm, and 1.00 μm, respectively.

Overall the SEM findings were consistent with the results of contact angle measurements. First of all, reproducibility of nanostructure was achieved on all polyolefins and PO/PFPE blends. Surfaces injection molded with the A mask showed high ordering as was expected from the structure of the mold insert. Surfaces injection molded with the B mask were less highly ordered, as was the mold insert itself. Surface structures prepared with the A mask also appeared to have a higher aspect ratio than those prepared with the B mask. These observations are in conformity with the results of the contact angle measurements: that is, the solid fraction of the surface was lower in surfaces injection molded with the A mask. Nanostructure was not always achieved over the entire surface. Images taken at lower magnification showed brighter and darker areas and nanostructure was found only in the bright areas. This difference is clearly evident in images G, H1, and H2 of Fig. 5. Image H1 has been taken from the left part and H2 from the right part of image G. Well-ordered nanostructure of high aspect ratio was found over the entire surface where, according to contact angle measurement, the solid fraction of the surface was less than 0.5 (bPE with A mask, and PP with A mask). In the other surfaces, nanostructure was not obtained over the entire surface, it was incomplete, or the aspect ratio was low, or all of those. We conclude that the SEM images confirm the results of the contact angle measurements.

4. Conclusions

Polyolefin surfaces were modified simultaneously chemically and structurally. Modifications were done by injection molding; liquid PFPE was added to the melt polyolefin and AAO mold insert was used to nanopattern surfaces. With the method described, the polyethylenes formed blends with PFPE, but not the polypropylene. Chemical modification increased the hydrophobicity of the polyethylenes, and the contact angle between water and the surface increased by about 10%. Nanostructuring had a marked effect on the contact angle between polyolefins and water. Especially with the A mask, a well-ordered high aspect ratio nanostructure was present over the entire surface, and the contact angle increased by about 25% while the solid fraction of the surface decreased to about 0.5. We conclude through these findings that our method allows the fabrication of injection-molded plastic components with improved hydrophobic properties.

Acknowledgements

The authors wish to thank Ms. Tuulia Korhonen for her help in fabricating the AAO masks.

References

[1] K. Kertész, Zs. Bálint, Z. Véresy, G.I. Márk, V. Lousse, J.-P. Vigneron, L.P. Biró, Photonic crystal type structures of biological origin: structural and spectral characterization, Curr. Appl. Phys. 6 (2006) 252–258.
[2] W. Barthlott, C. Neinhuis, Purity of the sacred lotus, or escape from contamination in biological surfaces, Planta 202 (1997) 1–8.
[3] B. Schulz, W.B. Frommer, A plant ABC transporter takes the lotus seat, Science 306 (2004) 622–625.
[4] J. Fresnais, J.P. Chapel, F. Poncin-Epaillard, Synthesis of transparent superhydrophobic polyethylene surfaces, Surf. Coatings Technol. 200 (2006) 5296–5305.
[5] S.R. Coulson, I. Woodward, J.P.S. Badyal, S.A. Brewer, C. Willis, Super-repellent composite fluoropolymer surfaces, J. Phys. Chem. B 104 (2000) 8836–8840.
[6] J.P. Youngblood, T.J. McCarthy, Ultrahydrophobic polymer surfaces prepared by simultaneous ablation of polypropylene and sputtering of poly(tetrafluoroethylene) using radio frequency plasma, Macromolecules 32 (1999) 6800–6806.
[7] K. Teshima, H. Sugimura, Y. Inoue, O. Takai, A. Takano, Ultra-water-repellent poly(ethyleneterephthalate) substrates, Langmuir 19 (2003) 10624–10627.
[8] A. Hozumi, O. Takai, Preparation of silicon oxide films having a water-repellent layer by multiple-step microwave plasma-enhanced chemical vapor deposition, Thin Solid Films 334 (1998) 54–59.
[9] H.Y. Erbil, A.L. Demirel, Y. Avci, O. Mert, Transformation of a simple plastic into a superhydrophobic surface, Science 299 (2003) 1377–1380.
[10] S. Shibuichi, T. Onda, N. Satoh, K. Tsujii, Super water-repellent surfaces resulting from fractal structure, J. Phys. Chem. 100 (1996) 19512–19517.
[11] T.A. von Werde, D.S. Germack, E.C. Hagberg, V.V. Sheares, C.J. Hawker, K.R. Carter, A versatile method for tunig the chemistry and size of nanoscopic features by living free radical polymerization, J. Am. Chem. Soc. 125 (2003) 3831–3838.
[12] C. Marzolin, S.P. Smith, M. Prentiss, G.M. Witesides, Fabrication of glass microstructures by micro-molding of sol–gel precursors, Adv. Mater. 10 (1998) 571–574.
[13] J. Bico, C. Marzolin, D. Quéré, Pearl drops, Europhys. Lett. 47 (1999) 220–226.
[14] C.L. Haynes, R.P. van Duyne, Nanosphere lithography: a versatile nanofabrication tool for studies of size-dependent nanoparticle optics, J. Phys. Chem. B 105 (2001) 5599–5611.
[15] J.-Y. Shiu, C.-W. Kuo, P. Chen, C.-Y. Mou, Fabrication of tunable superhydrophobic surfaces by nanosphere lithography, Chem. Mater. 16 (2004) 561–564.
[16] E. Schäffer, S. Harkema, M. Roerdink, R. Blossey, U. Steiner, Thermomechanical lithography: pattern replication using a temperature gradient driven instability, Adv. Mater. 15 (2003) 514–517.
[17] T. Textor, H. Schollmeyer, T. Bahners, E. Schollmeyer, Modification of low energy polymer surfaces by immobilization of fluorinated carboxylates with zirconium-based coupling agents, J. Appl. Polym. Sci. 94 (2004) 789–795.
[18] E. Bremius-Köbberling, A. Gillner, Laser structuring and modification of surfaces for chemical and medical micro components, Proc. SPIE 5063 (2003) 217–222.
[19] H. Pernot, M. Baumert, F. Court, L. Leibler, Design and properties of co-continuous nanostructured polymers by reactive blending, Nat. Mater. 1 (2002) 54–58.
[20] S.J. Ebbens, J.P.S. Badyal, Surface enrichment of fluorochemical-doped polypropylene films, Langmuir 17 (2001) 4050–4055.
[21] C.A. Harper, Modern Plastics Handbook, The McGraw-Hill Companies, New York, 2000, pp. 1.40–1.45, 1.60–1.63.
[22] E. Puukilainen, T.A. Pakkanen, Modification of surface properties of polyethylene by perfluoropolyether blending, J. Polym. Sci. Part B: Polym. Phys. 43 (2005) 2252–2258.
[23] J. Scheirs, Modern Fluoropolymers: High Performance Polymers for Diverse Applications, John Willey & Sons, Inc., Chichester, 1997, pp. 435–479.
[24] F. Li, L. Zhang, R.M. Metzger, On the growth of highly ordered pores in anodized aluminum oxide, Chem. Mater. 10 (1998) 2470–2480.

[25] H. Masuda, M. Satoh, Fabrication of gold nanodot array using anodic porous alumina as an evaporation mask, Jpn. J. Appl. Phys. 35 (1996) L126–L129.
[26] Z.L. Xiao, C.Y. Han, U. Welp, H.H. Wang, V.K. Vlasko-Vlasko, W.K. Kwok, D.J. Miller, J.M. Hiller, R.E. Cook, G.A. Willing, G.W. Crabtree, Nickel antidot arrays on anodic alumina substrates, Appl. Phys. Lett. 81 (2002) 2869–2871.
[27] T.T. Xu, R.D. Piner, R.S. Ruoff, An improved method to strip aluminum from porous anodic alumina films, Langmuir 19 (2003) 1443–1445.
[28] K. Nielsch, J. Choi, K. Schwirn, R.B. Wehrspohn, U. Gösele, Self-ordering regimes of porous alumina: the 10% porosity rule, Nano Lett. 2 (2002) 677–680.
[29] A.P. Li, F. Müller, U. Gösele, Polycrystalline and monocrystalline pore arrays with large interpore distance in anodic alumina, Electrochem. Solid State 3 (2000) 131–134.
[30] K. Liu, J. Nogués, C. Leighton, H. Masuda, K. Nishio, I.V. Roshchin, I.K. Schuller, Fabrication and thermal stability of arrays of Fe nanodots, Appl. Phys. Lett. 81 (2002) 4434–4436.
[31] X. Mei, D. Kim, H.E. Ruda, Q.X. Guo, Molecular-beam epitaxial growth of GaAs and InGaAs/GaAs nanodots arrays using anodic Al_2O_3 nanohole template masks, Appl. Phys. Lett. 81 (2002) 361–363.
[32] A.J. Yin, J. Li, W. Jian, A.J. Bennett, J.M. Xu, Fabrication of highly ordered metallic nanowire arrays by electrodeposition, Appl. Phys. Lett. 79 (2001) 1039–1041.
[33] N.S. Birenbaum, B.T. Lai, C.S. Chen, D.H. Reich, G.J. Meyer, Selective noncovaient adsorption of protein to bifunctional metallic nanowire surfaces, Langmuir 19 (2003) 9580–9582.
[34] T. Sehayek, A. Vaskevich, I. Rubinstein, Preparation of graded materials by laterally controlled template synthesis, J. Am. Chem. Soc. 125 (2003) 4718–4719.
[35] W. Lee, H.-I. Yoo, J.-K. Lee, Template route toward a novel nanostructured superionic conductor film; AgI nanorod/γ-Al_2O_3, Chem. Commun. 24 (2001) 2530–2531.
[36] M. Jung, H.-G. Kim, J.-K. Lee, O.-S. Joo, S.-I. Mho, EDLC characteristics of CNTs grown on nanoporous alumina templates, Electrochim. Acta 50 (2004) 857–862.
[37] M. Lahav, T. Sehayek, A. Vaskevich, I. Rubinstein, Nanoparticle nanotubes, Angew. Chem. Int. Ed. 42 (2003) 5576–5579.
[38] N. Beyer, Antireflective nanometersized surface structuring, VDI Berichte 1803 (2003) 17–21.
[39] T. Sawitowski, N. Beyer, S. Wagener, F. Schulz, Nanostructuring of surfaces using anodic alumina mask—methods, materials and properties, Nanotech 3 (2003) 1–4.
[40] F.M. Mirabella Jr., J.P. Coates, in: F.M. Mirabella Jr. (Ed.), Internal Reflection Spectroscopy: Theory and Applications, Marcel Dekker, Inc., New York, 1993, pp. 17–96.
[41] R.N. Wenzel, Resistance of solid surfaces to wetting by water, Ind. Eng. Chem. 28 (1936) 988–994.
[42] A.B.D. Cassie, S. Baxter, Wettability of porous surfaces, Trans. Faraday Soc. 40 (1944) 546–551.
[43] R.E. Johnson Jr., R.H. Dettre, Contact angle hysteresis, Adv. Chem. Ser. 43 (1964) 112–135, 136–144.
[44] D. Quéré, Rough ideas on wetting, Physica A 313 (2002) 32–46.
[45] A. Nakajima, K. Hashimoto, T. Watanabe, Recent studies on super-hydrophobic films, Monatshefte für Chemie 132 (2001) 31–41.
[46] M. Callies, Y. Chen, F. Marty, A. Pépin, D. Quéré, Microfabricated textured surfaces for super-hydrophobicity investigations, Microelectron. Eng. 78–79 (2005) 100–105.
[47] B. He, J. Lee, N.A. Patankar, Contact angle hysteresis on rough hydrophobic surfaces, Colloids Surf. A: Physicochem. Eng. Aspects 248 (2004) 101–104.